The "Normality" of El Niño

Gerrit Burgers

KNMI, De Bilt, The Netherlands

David B. Stephenson

Université de Paul Sabatier, Toulouse, France

Abstract. The amplitude of the El Niño-Southern Oscillation (ENSO) would be normally distributed if the coupled Pacific ocean-atmosphere were a linear system forced by Gaussian weather noise. Moment estimates of skewness and kurtosis demonstrate that this is not the case for monthly mean anomalies in Pacific sea surface temperatures during 1950-97. The noted predominance of El Niño events compared to La Niña events is related to the high skewness in the eastern Pacific. Skewness and kurtosis both exhibit an intriguing geographical variation from positive in the eastern to negative in the western Pacific. We have also examined Niño-3 indices generated by three climate models having widely different complexity. These exhibit a wide range of skewness and kurtosis values rather different from those found for the observations. Skewness and kurtosis can be used to diagnose non-linear processes and provide powerful tools for validating models, and for testing observed sea-surface temperatures for the presence of possible climate change.

1. Introduction

ENSO can be considered to be the response of a complex non-linear oscillator to stochastic shocks produced by weather events such as westerly wind bursts [*Philander*, 1990]. However, it is far from clear how much non-linearity there is in the coupled Pacific ocean-atmosphere system [*Neelin et al.*, 1998]. If the system were only very weakly non-linear, then one would expect the cumulative response to weather noise to be close to normally distributed. So, deviations from normality may be used as a tool to investigate the inherent non-linearity. For non-linear dynamical systems having multiple basins of attraction (regimes), the probability distribution can sometimes deviate so strongly from normality that multiple maxima appear (multimodality) [*Rivin and Tziperman*, 1997]. This study examines the deviations from normality in monthly mean anomalies of Pacific sea surface temperatures observed over 1950-97. In addition, ENSO Niño-3 indices produced by 3 different climate models are also analyzed and compared to the observations.

2. Observations

ENSO is often summarized by using area-averaged indices of sea surface temperatures across the tropical Pacific

ocean: Niño 12 (90-80W, 10S-EQ), Niño 3 (150-90W,5S-5N), Niño 3.4 (170-120W, 5S-5N), and Niño 4 (160E-150W, 5S-5N). This study investigates El Niño indices for the period January 1950 to December 1997 derived at NCEP [freely available from http://nic.fb4.noaa.gov/data/cddb]. Since January 1982, sea surface temperatures have been estimated using optimum interpolation of satellite, ship and buoy observations [*Reynolds and Smith*, 1994], whereas empirical orthogonal function (EOF) reconstruction was used prior to this period [*Smith et al.*, 1996]. Figure 1 shows histograms of the anomalies obtained by subtracting out the 1950-97 mean of each calendar month for each index. The distributions deviate from being normal, with notably the Niño-12 and Niño-3 indices strongly skewed to warm values, as discussed briefly by *Trenberth* [1997]. Out of the 576 monthly mean Niño-3 anomalies, 23 have been very warm ($> 2\sigma$), compared to 5 very cold ($< -2\sigma$). The western Pacific Niño-4 index is skewed to cold values and also has shorter tails and a broader maximum than a normal distribution.

One possible way to quantify deviations from normality is to examine the *skewness*, $\sqrt{b_1} = m_3/m_2^{3/2}$, and *kurtosis*, $b_2 - 3 = m_4/m_2^2 - 3$, where $m_k = \overline{(x - \overline{x})^k}$ is the k'th moment about the mean [*Mardia*, 1980]. Skewness towards high values means that high extremes are more probable than low extremes, while distributions that have no sharp central peak and clipped tails have a low kurtosis: a pure sinusoid limit cycle has a distribution with $b_2 - 3 = -1.5$. These statistics are presented for the observed ENSO indices in Table 1. For a large enough sample from a normal distribution, one expects $\sqrt{b_1} = 0$, and $b_2 - 3 = 0$. To test whether the indices are indeed normal, we have estimated confidence limits by calculating statistics for 10^5 Monte Carlo AR(1) red noise process realizations of the 576 month series. Serial correlations are taken into account by chosing the lag 1-month autocorrelation close to observed (0.92). The Monte Carlo results, shown in Figure 2, confirm that the Niño-12 and Niño-3 indices are not normally distributed. The simulations also reveal that kurtosis is positively correlated with the square of skewness ($r(b_2, b_1) = 0.47$). For this reason, we define a *reduced kurtosis* as $b_2' = b_2 - 3 - 1.5b_1$. Low values of reduced kurtosis can indicate the presence of non-linear chaotic or periodic regimes in systems with skewed distributions (cf. the discussion in [*Rivin and Tziperman*, 1997]. With b_2' as ordinate, the cloud of Monte Carlo points in Figure 2 is almost isotropic. It is apparent from Figure 2 that the Niño-3 and Niño-12 values lie outside the 95% confidence limit enclosing the cloud of normally distributed red noise points. The deviation from normality is due to the large values of skewness. The reduced kurtosis values are
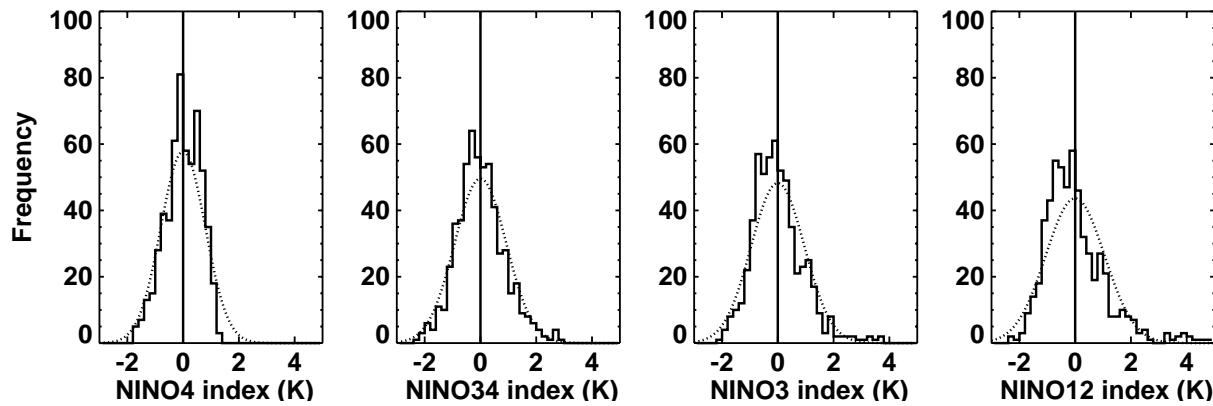
Figure 1. Histograms of the monthly mean Niño index anomalies from 1950–97. For comparison, normal distributions with the observed standard deviation are drawn (dashed line). The mean anomalies are zero by definition. A bin width of 0.2°C was used.

generally small. This suggests that the gamma distribution with $b_2 - 3 = 1.5b_1$ may provide a good fit to the distributions [*Stephenson et al.*, 1998]. If one considers that the variance of the signal depends on the calendar month, by testing on anomalies standarized on monthly variances, it is found that the Niño-4 reduced kurtosis is significantly lower than normal.

Comparing $(\sqrt{b_1}, b_2')$ of the Niño-3 index for the period 1950–91 in different SST analyses gives (0.60, 0.2) for the NCEP analysis, (0.40, 0.1) for the GISST2.2 analysis [*Rayner et al.*, 1996] and (0.59, 0.2) for the Kaplan analysis [*Kaplan et al.*, 1998], in reasonable agreement. Skewness, and especially kurtosis, vary depending on the period selected, in particular on whether large events are included or not. Also, for a given period, kurtosis, and to a lesser extent skewness, are harder to estimate when data are sparse, as before 1950.

Skewness and kurtosis of the Niño indices decrease markedly when going from east to west across the Pacific (Table 1). Looking in more detail at the geographical variations, we plot the skewness and kurtosis of monthly mean anomalies of EOF interpolated SST fields for 1950–97 [*Smith et al.*, 1996] in Figure 3. Figure 3a confirms that skewness goes from values exceeding 1.2 in the eastern Pacific to values of -0.4 in the western Pacific.

Table 1. Statistics for monthly-mean anomalies of ENSO indices estimated by NCEP over the period 1950–97; up to 1982 an EOF reconstruction [*Smith et al., 1996*] is used, from 1982 the OI product [*Reynolds and Smith, 1994*]. S.Dev is the standard deviation, r_1 is the lag 1-month autocorrelation, $\sqrt{b_1}$ is the skewness, $b_2 - 3$ is the kurtosis, and b_2' is the reduced kurtosis. Also shown are the 95% confidence limits for 576-month sections of an AR(1) red noise process with $r_1 = 0.92$. Values outside these 95% confidence limits are in bold face.

Index	S.Dev	r_1	$\sqrt{b_1}$	$b_2 - 3$	b_2'
Niño 12	1.11°C	0.90	**1.34**	**2.83**	0.14
Niño 3	0.91°C	0.92	**0.86**	**1.59**	0.48
Niño 3.4	0.86°C	0.93	0.37	0.48	0.27
Niño 4	0.63°C	0.92	-0.35	-0.38	-0.56
AR(1)	—	0.92	±0.5	±0.8	±0.7

Skewness is a powerful diagnostic for validating climate data sets and could be used more frequently for this purpose. For example, the global skewness map for the OI analyses 1982-97 contains an eye-catching bulls-eye pattern to the west of Indonesia (with $\sqrt{b_1}$ less than -2.5) due to erroneous satellite estimates of SSTs in 1994 and 1997 caused by excessive smoke from Indonesian forest fires (personal communication, Dick Reynolds).

3. Model results

Skewness and kurtosis have also been estimated for Niño-3 indices generated by three climate models of widely different complexity. The NCAR Climate System Model (NCAR CSM) is a state-of-the-art global coupled ocean-atmosphere model that has been run for 300 years without applying any correction to the air-sea fluxes [*Boville and Gent*, 1998; *Liang and Wang*, 1998]. The Cane-Zebiak model (CZ) is a coupled model of intermediate complexity for the Pacific
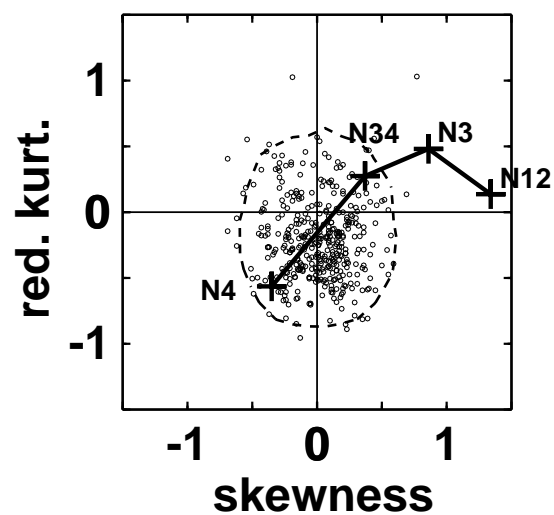

Figure 2. Scatter plot of reduced kurtosis versus skewness estimated for the observed Niño indices over 1950–97 (labeled +). The cloud of points marks values obtained for 400 Monte Carlo realizations of an AR(1) red noise process, with a lag-1 correlation of 0.92. The dashed contour encloses 95% of the Monte Carlo points.
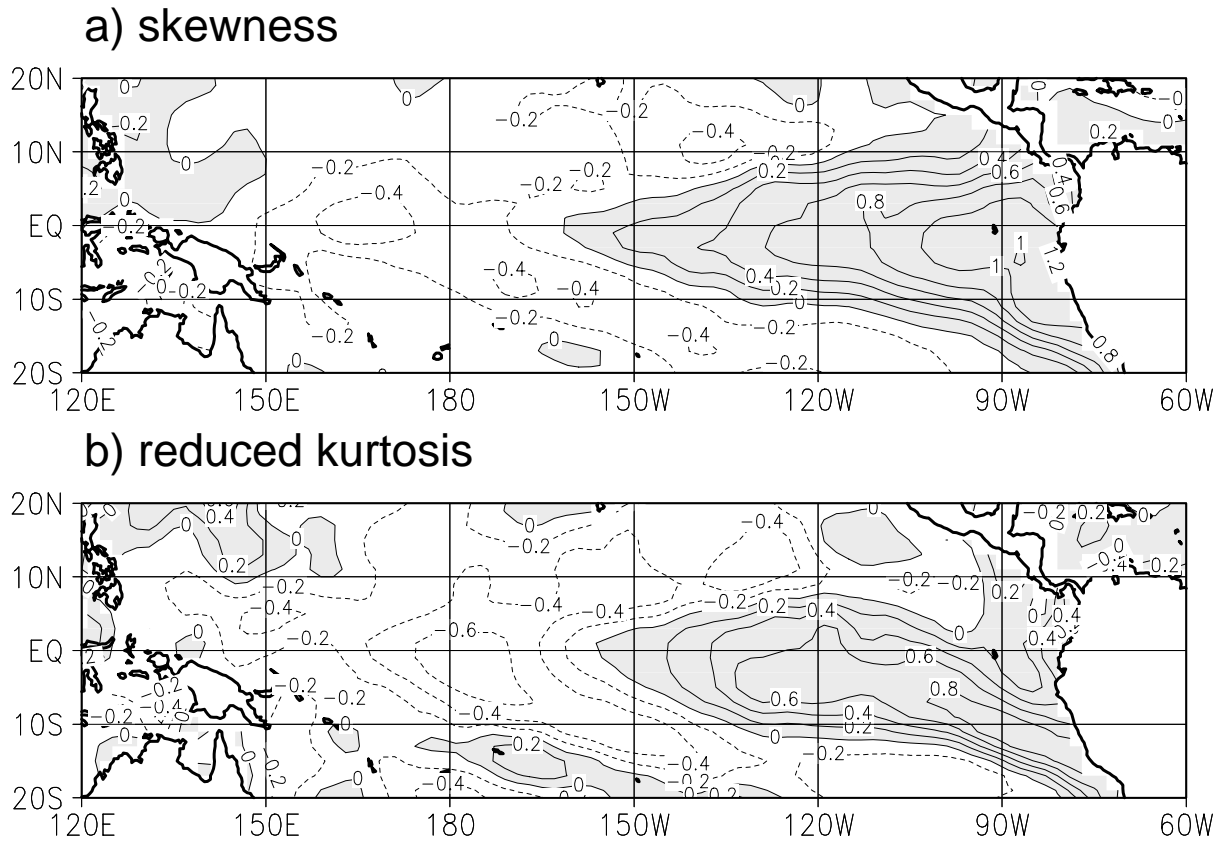
a) skewness

b) reduced kurtosis

Figure 3. Spatial distribution of a) skewness, and b) reduced kurtosis for the observed monthly mean sea surface temperature anomalies in the Pacific ocean from 1950–97. Note the marked difference between the eastern and western Pacific.

that has been used in many studies of ENSO [*Zebiak and Cane*, 1987]. Because of its speed, we were able to make a long run of 20000 years. TSCJ is a one-variable conceptual model of ENSO and its interaction with the annual cycle proposed by [*Tziperman et al.*, 1994], that we used to generate a very long 10^5 year run.

The model skewness and kurtosis values differ widely from one another (Table 2), and also from the observed values (Figure 4). NCAR CSM has small values of skewness and kurtosis not significantly different from normally distributed, that suggests the model is underestimating the non-linearity in ENSO. This is likely since the model also

severely underestimates the amplitude of the ENSO variations. The CZ model gives a positively skewed Niño-3 index, as the observed index. The model also gives strongly negative reduced kurtosis, unlike observed. However, there is so much spread in the skewness and kurtosis values of the 400 realizations that one can not state with certainty that they are incompatible with the observed values. The TSCJ model gives negative skewness and kurtosis values of opposite sign to those observed for Niño 3. These arise in this model from an overly strong interaction of ENSO with the annual cycle, and can be made less negative by adding noise to the model as was proposed by [*Stone et al.*, 1998]. Low
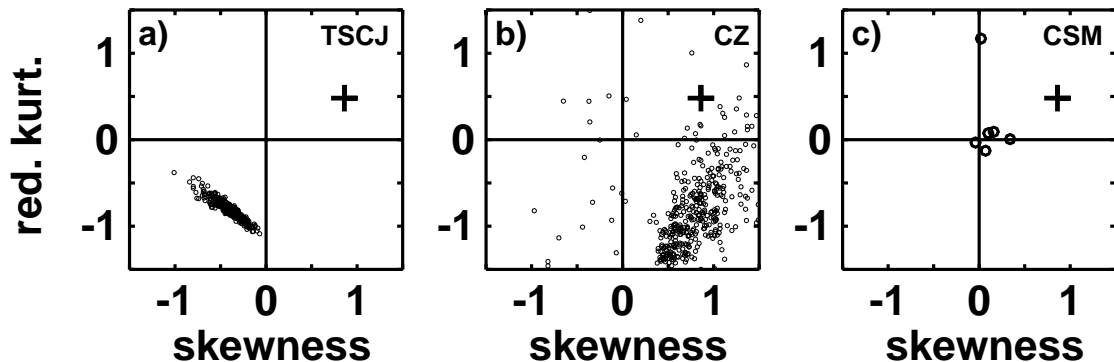

Figure 4. Scatter plot of reduced kurtosis versus skewness of the Niño-3 index in sections of 576 months generated by (a) TSCJ conceptual model, (b) CZ intermediate model, and (c) NCAR CSM global coupled climate model. The value for the observed Niño-3 index over the period 1950–1997 is also shown (labeled +).

Table 2. Statistics estimated for monthly Niño-3 time series produced by three different dynamical models, and for the observations 1950-97. The statistics have been averaged over N independent 576-month samples.

Source	N	S.Dev	r_1	$\sqrt{b_1}$	$b_2 - 3$	b_2'
CSM	6	0.46°C	0.79	0.11	0.24	0.19
CZ	400	1.13°C	0.98	0.79	0.48	-0.75
TSCJ	2000	—	0.98	-0.39	-0.56	-0.82
Observed	1	0.91°C	0.92	0.86	1.59	0.48

values of reduced kurtosis, as in the TSCJ and CZ model, can point to the presence of non-linear chaotic or periodic regimes (cf. [*Rivin and Tziperman*, 1997]). The observed Niño-3 index gives no such indication.

4. Concluding Remarks

The issue of whether the amplitude of El Niño SST anomalies are normal has several aspects. In the upwelling region in the eastern Pacific, SSTs deviate significantly from normality by being positively skewed [thereby helping to explain why Peruvian fisherman first discovered El Niño and not La Niña!]. However, in the warm pool region in the western Pacific, SSTs are negatively skewed, also the reduced kurtosis in the western Pacific is lower than in the eastern Pacific. In the central Pacific, near $150-160W$, both skewness and kurtosis have almost normal distribution values, and therefore the distribution of the Niño-3.4 index is close to normal. Other ENSO indices, such as the Southern Oscillation sea-level pressure index are also found to be approximately normally distributed [*Stephenson*, 1997].

Largest SST skewness occurs in the upwelling region in the eastern equatorial Pacific, where the thermocline is already close to the surface, and therefore more difficult to obtain much colder than warmer SSTs. The negative skewness in the warm pool region is most probably caused by SSTs saturating at 30°C due to non-linear radiative-convective greenhouse feedbacks. Thus local non-linear saturation could explain much of the non-normality of ENSO.

This study has demonstrated that three different dynamical models give widely differing results, yet that none is able to reproduce the observed skewness and kurtosis. This suggests that the climate models are failing to capture correctly the non-linear aspects of ENSO. Skewness and kurtosis are also powerful tools for validating and comparing gridded analyses of historical SSTs - some of which also severely underestimate the extreme behaviour in SSTs.

The fact that ENSO indices such as Niño 3 deviate significantly from normality has important implications for ENSO forecasting, for example forecasts from models that are less skew than observed (e.g. linear statistical models) will underestimate extreme El Niño events. Also, non-normality can easily give the impression of non-stationarity in time series and should therefore also be taken into account when assessing whether global warming has occurred [*Trenberth*, 1997]. It has been suggested [*Timmermann*, 1998; *Timmermann et al.*, 1998] that the skewness of the Niño-3 index may change in the advent of enhanced greenhouse warming. It is therefore of interest to continue monitoring carefully the skewness and kurtosis of observed and modeled SSTs.

References

B.A. Boville and P.R. Gent, The NCAR climate system model, version one, *J. Clim., 11,* 3518–3528, 1998.

A. Kaplan, M.A. Cane, Y. Kushnir, A.C. Clement, M.B. Blumenthal and B. Rajagopalan, Analyses of global sea surface temperature 1856-1991, *J. Geophys. Res., 103,* 18567–18589, 1998.

X.-Z. Liang and W.-C. Wang, The observed fingerprint of 1980–1997 ENSO evolution in the NCAR CSM equilibrium simulation, *Geophys. Res. Lett., 25,* 1027–1030, 1998.

K.V. Mardia, Tests of univariate and multivariate normality, in *Handbook of Statistics Vol. 1*, edited by P.R. Krishnaiah, pp. 279–320, North Holland Publishing Company, Amsterdam, 1980.

J.D. Neelin, D.S. Battisti, A.C. Hirst, F.F. Jin, Y. Wakata, T. Yamagata, and S. Zebiak, ENSO Theory, *J. Geophys. Res., 103,* 14261–14290, 1998.

S.G.H. Philander, *El Niño, La Niña and the Southern Oscillation,* 293 pp., Academic Press, San Diego, Calif., 1990.

N.A. Rayner, E.B. Horton, D.E. Parker, C.K. Folland, and R.B. Hackett, Version 2.2 of the Global sea-Ice and Sea Surface Temperature (GISST) data set 1903–94, *Hadley Centre TN-74,* 34 pp., Hadley Centre, Bracknell, United Kingdom, 1996.

R.W. Reynolds and T.M. Smith, Improved global sea surface temperature analyses using optimum interpolation, *J. Clim., 7,* 929–948, 1994.

I. Rivin and E. Tziperman, Linear versus self-sustained interdecadal thermohaline variability I: Model, *J. Phys. Oceanogr., 27,* 1216–1232, 1997.

T.M. Smith, R.W. Reynolds, R.E. Livezey, and D.C. Stokes, Reconstruction of historical sea surface temperatures using empirical orthogonal functions, *J. Clim., 9,* 1403–1420, 1996.

Stephenson, D.B., Correlation of Spatial Climate/Weather Maps and the Advantages of using the Mahalanobis Metric in Predictions, *Tellus 49A,* 513–527, 1997.

Stephenson, D.B., K. Rupa Kumar, F.J. Doblas-Reyes, J.F. Royer, F. Chauvin, and S. Pezzuli, Extreme daily rainfall events and their impact on ensemble forecasts of the the Indian monsoon, *Mon. Weather Rev.,* 1998, (in press).

L. Stone, P.I. Sapirin, A. Huppert, and C. Price, El Niño chaos: The role of noise and stochastic resonance on the ENSO cycle, *Geophys. Res. Lett., 25,* 175–178, 1998.

A. Timmermann, J. Oberhuber, A. Bacher, M. Esch, M. Latif and E. Roeckner: ENSO response to greenhouse warming, *MPI Report 251,* 13 pp., MPI, Hamburg, 1998.

A. Timmermann, Detecting the nonstationary response of ENSO to Greenhouse warming, *J. Atm. Sc.,* 1999, (in press).

K.E. Trenberth: The definition of El Niño, *Bull. Am. Meteorol. Soc., 78,* 2771–2777, 1997.

E. Tziperman, L. Stone, M.A. Cane, and H. Jarosh: El Niño chaos: Overlapping of resonances between the seasonal cycle and the Pacific ocean-atmosphere oscillator, *Science 263*, 72–74, 1994.

S. Zebiak and M.A. Cane: A model El Niño-Southern Oscillation, *Mon. Weather Rev., 115,* 2262–2278, 1987.

G. Burgers, KNMI, P.O.B. 201, 3730 AE De Bilt, The Netherlands (e-mail: burgers@knmi.nl)

D.B. Stephenson, Laboratoire de Statistiques et Probabilités, Université de Paul Sabatier, 118 route de Narbonne, 31061 Toulouse, France (e-mail: stephen@cict.fr)